Published in final edited form as:

Circ Arrhythm Electrophysiol. 2017 July ; 10(7): . doi:10.1161/CIRCEP.117.004743.

Imaging-Based Simulations for Predicting Sudden Death and Guiding VT Ablation

Natalia A. Trayanova, PhD[1], **Farhad Pashakhanloo, PhD**[1], **Katherine C. Wu, MD**[2], and **Henry R. Halperin, MD**[2,3]

[1]Institute for Computational Medicine & Department of Biomedical Engineering, Johns Hopkins University, Baltimore, MD

[2]Division of Cardiology, Department of Medicine, Johns Hopkins Medical Institutions, Baltimore, MD

[3]Departments of Radiology and Biomedical Engineering, Johns Hopkins University, Baltimore, MD

Keywords

arrhythmia; ventricular tachycardia; myocardial infarction; cardiac ablation; LGE-CMR; image-based simulations

Journal Subject Terms

Arrhythmias; Catheter Ablation and Implantable Cardioverter-Defibrillator; Sudden Cardiac Death; Myocardial Infarction; Magnetic Resonance Imaging (MRI)

Introduction

Simulation-driven engineering has put rockets in space, airplanes in the sky, and self-driving cars on the road. Computational approaches have also contributed to advancements in clinical medicine and human health[1–3]. In the arena of cardiac care, the recent emphasis on personalized medicine has provided a significant impetus for the development of predictive approaches combining imaging and computational modeling that can be applied to the diagnosis and treatment of heart rhythm disorders. A major advance in this direction is the creation and translation into clinical practice of novel imaging- and simulation-based strategies for predicting an individual's risk of sudden cardiac death (SCD) and for the non-invasive planning of optimal personalized anti-arrhythmia therapies. Clinical decisions regarding the stratification of patients for SCD risk resulting from arrhythmia and for determining the optimal targets for anti-arrhythmia ablation therapies could greatly benefit from such targeted developments since current approaches, although life-saving, remain sub-

Correspondence: Natalia Trayanova, PhD, Institute for Computational Medicine, Johns Hopkins University, 3400 N. Charles Street, Baltimore, MD 21218, Tel: 410-516-4375, Fax: 410-516-5294, ntrayanova@jhu.edu.

Disclosures: None.

optimal, often increase the burden on the healthcare system, and could lead to increased patient morbidity.

SCD resulting from ventricular arrhythmias is a leading cause of death in the industrialized world, particularly among patients with prior myocardial infarction[4]. For patients at high risk of SCD, mortality is reduced by the prophylactic insertion of implantable cardioverter defibrillators (ICDs)[5]. To determine the level of SCD risk, clinical cardiology practice still relies on the 'one-size- fits-all' metric of left ventricular ejection fraction (LVEF) below 35% to identify high-risk patients. Mechanistically, in hearts with structural disease, arrhythmia results from the heterogeneously distributed remodeled tissue, which can promote the initiation and maintenance of electrical instability. Global LVEF poorly reflects these mechanistic factors and, hence, its use to determine the level of SCD risk and stratify patients for ICD implantation results in a low rate of appropriate ICD device therapy, only 5% per year[6]. Thus, many patients are exposed to ICD risks—infections, device malfunctions and inappropriate shocks—without deriving any health benefit[7]. Further, the LVEF metric only targets a relatively small subgroup of individuals at high risk for SCD, failing to identify the majority of SCD victims (i.e. the Myerburg conundrum). Personalized risk assessment could ensure life-saving timely intervention in patients at high risk, while limiting unnecessary ICD implantations in patients with low risk.

In patients with ventricular tachycardia (VT), particularly those with structural disease (e.g. myocardial infarction, MI), catheter-based ablation offers the possibility of permanent cure. However, it is associated with modest levels of success in eliminating infarct-related VT, 50–88%[8,9], and with complication rates as high as 8% of the treated population[10]. The insufficient efficacy of the procedure stems from limitations in current voltage and pace mapping techniques used to identify the target locations for ablation[11–15]. There is a need for new approaches that can result in swift and accurate identification of optimal ablation targets and thereby improve the efficacy of and increase the tolerance for the therapy and reduce post-procedure complications. Finally, since early use of VT ablation post-infarction has been recently shown to result in much improved patient outcomes (SMASH-VT Trial[16]), an accurate and easily executed VT ablation will lead to significant broadening of the therapeutic potential of the procedure.

Novel non-invasive imaging- and simulation-based strategies have been recently developed to address these clinical needs in patients with structural heart disease. They are based on personalized information regarding the distribution of structural remodeling in the patient's ventricles as obtained from clinical imaging scans and on the biology and physics of heart cells and the electrical current flow patterns through the cardiac syncytium, resulting in the construction of a virtual replica of the patient's heart – i.e. the patient's virtual heart. Using a virtual heart, the patient's unique lethal heart rhythm disorder can be studied *in silico*, and personalized treatment devised. Researchers can poke and prod the virtual organ in ways that are simply not possible with a flesh-and-blood heart. The hope is that with such models at the patient bedside, therapies could be improved, invasiveness of diagnostic procedures minimized, and health-care costs reduced.

The goal of this article is to review recent developments of the personalized virtual-heart methodology in determining risk of SCD and predicting the optimal targets for infarct-related VT ablation in myocardial infarction (MI) patients. We present the methodology fundamentals based on cardiac imaging and computational modeling, outlining important assumptions, followed by a review of validation studies. We discuss the potential impact this approach could have on treatments for arrhythmias and how this can bring personalized medicine to the arena of cardiac care.

How to Construct a Virtual Heart

For both SCD risk stratification and ablation planning, a three-dimensional (3D) computer model of MI patient's individual heart is constructed from contrast-enhanced clinical cardiac magnetic resonance imaging (CMR) data. The heart model incorporates the patient's ventricular geometry and MI structural remodeling (the personalized part of the model) as well as electrical functions from the sub-cellular to the organ level (based on the known biology of myocytes and the physics of current flow). The model is thus capable of representing the interplay between abnormal MI myocardial structure and electrical instability in the heart that results in the generation and maintenance of ventricular arrhythmias. A virtual multi-site delivery of electrical stimuli from a large number of ventricular locations at different distances to remodeled tissue ensures that the ventricular substrate's propensity to develop infarct-related ventricular arrhythmias can be comprehensively evaluated.

Personalized Geometrical Model Construction

Patient-specific geometrical models of 3D ventricular structure are reconstructed from the late gadolinium enhanced (LGE)- CMR scans (Figure 1). For information regarding CMR acquisition, please refer to the methods description in Arevalo et al[17] For each patient, the myocardial boundaries in the CMR stack are contoured using landmark points and the patient-specific 3D ventricular wall geometry is reconstructed[18]. The myocardial regions are then classified as infarcted and non-infarcted by means of signal thresholding. The cut-off thresholds were determined on the basis of a percentage of the maximum intensity of the scar (such as full-width half-max method)[17]; alternatively, a methodology based on standard deviations above the remote normal tissue could be used. Although the ICD artifact can obscure part of the image, the geometry of the ventricles could nonetheless be reconstructed from the partially missing data using landmark-based interpolations[19]. The presence of ICD shadow in the scar area, however, could in some cases severely affect the assessment of the scar distribution. The application of a wideband LGE-MRI[20] has shown promising results in suppressing the ICD artifact in the heart, and could be used in future applications of the "virtual heart" imaging-simulation methodology.

Previous research[21] has indicated that the presence and extent of the infarct border zone (termed also gray zone, GZ, because of its intermediate CMR signal intensity) contributes to arrhythmia propensity, thus pixels belonging to infarcted tissue are further sub-classified as scar or GZ. In creating the patient's heart model, the 3D geometries of the infarct zones are segmented[22] and reconstructed[23], and then merged with the ventricular geometry. Next, the

3D finite element mesh is generated using an approach developed for image-based meshes[24]. Each finite element ventricular mesh has an average resolution of 350μm, as needed to adequately resolve wavefront propagation[25]. Mesh generation is automatic, and produces boundary-fitted, locally refined and smooth conformal meshes, preserving the boundaries of scar and GZ, as reconstructed from the MRI.

The final step in model construction is determining the fiber orientation in each element of the ventricular mesh. Patient myocardial fiber orientations cannot be currently acquired *in vivo*, although a recent study demonstrated significant progress towards *in-vivo* diffusion-tensor (DT) MRI[26]. As an alternative approach, two methodologies have been developed to date for assigning fiber orientations on the basis of the individual geometry of the ventricles. The first is an atlas-based approach using *ex vivo* MRI and DT-MR images of a human heart (the atlas)[27]. Using image transformation algorithms, the atlas ventricular geometry is deformed to match that of the patient. The same deformation field is then applied to the atlas fiber orientations to obtain an estimate of patient fiber orientations. Computational simulations of ventricular activation maps and pseudo-ECGs in sinus rhythm and VT in animal hearts[27] closely matched those using DT-acquired fiber orientations, validating the approach. The approach has been used to assign fiber orientations in a study of two patient-specific ventricular models[28]. The downside of the methodology is its computational expense, limiting the approach in cases where time is crucial, as in ablation targets prediction where the time period between CMR scan and procedure is 24 hours or less. A much faster rule-based fiber orientation estimation has been developed[29], also assigning fiber orientations based on the individual ventricular geometry; it interpolates fiber orientations based on rules derived from fiber orientation histological and DT-MRI data. Bayer et al[29] compared simulations of ventricular activation in a model with rule-based fibers to those in the same geometrical model but with DTI-derived fiber orientation. The results demonstrated that activation patterns were nearly indistinguishable, with relative differences <6% and positive correlations >0.99, indicating a robust algorithm.

After fiber orientations were assigned, the corresponding GZ and scar ‘masks’ are superimposed. The scar is considered non-conductive, thus no electrophysiological parameters, including anisotropy arising from fiber orientation, is of any consideration there. Fiber orientation in GZ, as estimated by the methodology described above, was the subject of concern, as there could be some level of fiber rearrangement not captured by those methodologies. The high-resolution imaging study by by Pashakhanloo et al[30] who used sub-millimeter-resolution DT and LGE-MRI on a clinical scanner to examine the detailed organization of the infarct structure in the ventricles. The study demonstrated that the epi-to-endo progression of the diffusion tensor primary eigenvector is preserved in infarcted parts of the wall in human (Figure 2) and in porcine hearts, justifying the adoption of a rule-based approach to fiber orientation estimation in the zone of infarct.

Non-personalized Electrophysiological Model Parametrization

Once the ventricular mesh is generated, average human cell and tissue electrophysiological properties are assigned to scar, GZ and non-infarcted tissue. Scar region is considered electrically non-conductive, while finite elements that belonged to non-infarcted tissue and

GZ are assigned regionally-uniform human ventricular cell action potential dynamics. Remodeled GZ ionic properties are represented by modifying the human action potential model with data from experimental recordings; detail can be found in recent publications[17,31–33], showing GZ action potentials characterized by longer durations, decreased upstroke velocity and decreased peak amplitude. Tissue properties representing human ventricular cell-to-cell electrical communication are also assigned to the non-infarcted and GZ regions, with values of conductivities as described previously[17]. GZ region is characterized with a decrease in transverse conductivity to reflect connexin-43 remodeling in the infarct border zone.

The propagation of electrical activity in a virtual heart is simulated by solving, using the finite element method, a reaction-diffusion equation representing the spread of current in the ventricular myocardium, together with the ordinary differential and algebraic equations representing myocyte membrane dynamics at each node in the mesh[34]. This approach has been experimentally validated[35–37] and used in a number of mechanistic arrhythmia studies[38–40].

The approach to personalize virtual hearts with respect to only heart geometry and regional distribution of structural remodeling, and not with respect to the values of electrophysiological properties, as reviewed here, stands apart from previous attempts at image-based modeling of ventricular function. In such studies personalization of electrophysiological properties was also carried out, either in porcine models[41] or in small studies of 1 to 7 patients[42,43], based on voltage measurements, demonstrating good correspondence between simulation results and VT circuit measurements. Instead, the approach reviewed here enables the construction of a virtual heart model based on non-invasive information only. It is suitable for the non-invasive assessment of the ventricular substrate arrhythmogenic propensity in patients with *structural heart disease*, where structural remodeling plays a major role in arrhythmogenicity. In its current form, the virtual heart approach lends itself to applications such as the prediction of the infarct-related VT ablation targets and post-MI risk stratification for arrhythmia. As the approach evolves, the expectations are that tests will be performed to determine whether additional personalization (presence of antiarrhythmic drugs; genetic information, etc.) can further improve its predictive capability and broaden its applicability to arrhythmias resulting from different heart diseases.

Protocol for evaluating the arrhythmogenic propensity of the ventricular substrate

To evaluate the arrhythmogenic propensity of the structurally-remodeled substrate, each post-MI virtual heart is subjected to pacing from multiple locations to elicit reentrant arrhythmias; information about the specific pacing protocol can be found in Arevalo et al[17]. In this way the potential of the disease-remodeled ventricles to cause degeneration of propagation into arrhythmia following premature beats that originate at different locations in the heart can be fully assessed. Since all pacing sites are assigned automatically, typically using AHA nomenclature for segment locations, the number of pacing sites uniformly distributed throughout the left and right ventricles (LV and RV) can be chosen. In recent publications[17,33], each virtual heart was paced from at least 19 different locations. The

distribution of pacing sites throughout the ventricles, and particularly the LV, ensures that the protocol covers a large range of possibilities for potential sites at which ectopic foci could emerge and captures all the possible arrhythmias that could arise from the given structural remodeling distribution.

Validation of Post-MI Arrhythmia Modeling

Do arrhythmias calculated by a virtual heart, as described above, mimic the actual arrhythmias in the patient? This question is very difficult to address in the clinical setting, as specific pacing locations (typically in the RV) during an electrophysiological study are difficult to be exactly reproduced in the model. Given a distributed morphology of GZ and scar and the propensity for arrhythmogenesis, often even small differences in pacing locations between a clinical study and model could result in a different morphology of the elicited arrhythmia, making such comparisons difficult. To do so, a prospective validation study needs to be carefully designed to ensure the pacing sites could be matched. Initial attempts in this direction have already been made[44], but a larger patient cohort is needed to confirm model predictions in the clinical setting.

Validation of the virtual heart approach has been instead carried out in a swine model. Deng et al[32] used sock epicardial data for infarct-related VT, obtained from four swine hearts, and demonstrated that models reconstructed from clinical-resolution MRI data of the corresponding hearts were able to predict fairly accurately the morphology of each VT circuit and its organizing center (for example, isthmus). Figure 3 shows VT results from two of the swine models and the corresponding experimentally-recorded epicardial map. The simulations also reveal the nature of the transmural ventricular activity that manifests itself into epicardial activity mimicking the experimental findings. Furthermore, the study also compared models reconstructed from high-resolution (Hi-res) *ex-vivo* MRI of the same swine hearts with those of clinical resolution (Lo-res). The organizing centers of the reentrant circuits induced in the Lo-res models closely matched those in the Hi-res models (difference of 11.3 ± 4.1 mm). Since a given location is targeted by several ablations, the predicted organizing centers for the VT circuits in the Low-res models were, for all practical purposes, co-localized to the “true” VT circuit location predicted in the Hi-res models. Since clinical ablation usually involve the delivery of multiple lesions in one area, the study concluded that MRI-based computer models of MI hearts could indeed provide a unique opportunity to predict and analyze VTs resulting from specific infarct architectures.

Deng et al[32] demonstrated that the geometrical morphologies of scar and GZ, as well as the representation of differences in electrophysiological properties in non-infarcted tissue and GZ have a primary role in determining VT inducibility and the location(s) of its organizing center. This is consistent with the findings by Arevalo et al[31] where a parameter sensitivity analysis of the GZ model representation was conducted. The research found, using post-MI canine ventricles models, that inclusion of small scar heterogeneities in a physiological density did not alter inducibility of infarct-related VT or its morphology. In the study, first micro-regions of scar were randomly distributed throughout the GZ at varying densities. Following pacing from a number of sites, the locations of the resulting organized centers of reentrant activity (filaments) were compared to those in the corresponding homogeneous GZ

model. Incorporation of micro-regions of scar in the GZ (Figure 4A shows the 60% case) resulted in some conduction slowing within the GZ (Figure 4B). For the typical heterogeneous cases where GZ was composed of up to 40% scar, all induced VT morphologies were fully identical to the control, and the filaments remained in the same spatial position. The study next incorporated random micro-regions at increasing density in the GZ, but this time these were composed of normal myocardium. The simulations revealed that models with unchanged GZ conductivities but GZ composition incorporating up to 80% normal tissue exhibited the same VT morphology as in control; VT cycle lengths also did not differ significantly from the control. This study provided the justification for the use of uniform GZ properties in the virtual heart models, and established that even fairly substantial changes in model parameters had minimal effects on model predictions.

Feasibility of Using Virtual Hearts to Estimate Ablation Targets

Figure 5 presents the concept of using patient-derived virtual hearts to predict optimal ablation targets. It substitutes the invasive mapping to determine the arrhythmia critical pathways with evaluation of model VT circuits. From the simulated VTs, ablation targets can be determined, and then implemented in the virtual heart as non-conductive lesions to simulate ablation and determine whether the lesions result in VT non-inducibility from any pacing site. It is possible that following ablation new VT circuits could be formed in the virtual heart. They will then be evaluated and the appropriate ablation targets determined. The process can be repeated until complete non-inducibility is achieved. The resulting set of ablation targets could then be loaded into the 3D electro-anatomical mapping system, so that the ablation catheter is navigated during the procedure to the model-predicted targets. VT ablation would then be swift and precise, eliminating VT circuits with minimum lesions and maximum chance of VT non-inducibility.

While such an approach has not yet been prospectively implemented clinically, initial steps towards it have already been made. Ashikaga et al[45] conducted a retrospective study in 13 patients who had pre-ablation MRI for infarct-related VT ablation. Simulations with patient-specific models induced VTs and estimated targets according to the simulated circuits. Comparisons between simulation results and clinical recordings were made in 11 patients. In 5 patients, VT circuits were of the figure-of-eight reentry pattern (Figure 6, A and B). The central common pathway was located over the GZ or the superficial layer of the viable myocardium over the scar. In this type of circuit in the virtual hearts, the target region was estimated to be an area bordered by two facing lines of conduction block that compose the isthmus (Figure 6, A and B, green area in right-most column). An ablation line between the two facing conduction block lines was expected to prevent VT recurrence, and the minimum length of this hypothetical ablation line (i.e. narrowest isthmus width) was quantified. In 7 patients, virtual heart VT circuits were of unidirectional reentry pattern (Figure 6C), and the target region was estimated to be a triangular area that connects the closer end of the conduction block line to an adjacent anatomical barrier (e.g. mitral annulus); the minimum length of this hypothetical ablation line was also quantified.

The comparison between the estimated ablations in simulations and in the standard clinical approach showed that these are highly consistent (82%); in 9 of 11 cases, ablation within the

estimated target region was associated with acute success (n = 8) and ablation outside the estimated target region was associated with failure (n = 1). The results of this study indicated that virtual-heart simulations could be used to estimate ablation targets. The simulation results also determined that the narrowest width of the target region that an ablation line should span to prevent VT recurrence was relatively small (5.0 ± 3.4 mm). This indicated that the pre-procedural estimation of the location and the size of the target region by simulation would likely help reduce procedure time.

While the study[45] did not perform model ablation and post-ablation tests of VT non-inducibility, it demonstrated that this approach could have value in the clinic. To fully ascertain the potential of the virtual heart approach in predicting the optimal ablation targets, research needs to demonstrate its ability to determine, using a verified operator-independent algorithm, the optimal ablation targets that terminate all VTs, rather than applying the currently clinical decision making process to the VT circuits in the virtual heart. Such an approach was recently undertaken in predicting the ablation targets for macro-reentrant atrial tachycardia[46], and could also be applied to infarct-related VT ablation. Non-inducibility studies following the *in silico* ablation will need to also be conducted to verify that no new VTs arise post-ablation, and if they do, to determine the additional ablation targets. Importantly, the utility of the approach can only be verified in a prospective study, requiring the overcoming of technical barriers associated with merging the predicted targets with the 3D electroanatomical navigation system. Finally, research will need to validate that the lesions specified by the *in silico* studies can actually be generated in a patient. Imaging methods can validate this directly. It has been shown that the extent of ablation lesions can be determined with late gadolinium enhanced MRI, as well as with non-contrast methods, during or just after an actual ablation procedure[47]. Prospective studies are needed, therefore, to compare directly the results from *in silico* predictions, with those of actual ablation, where lesion extent is quantified with MRI.

Using Virtual Hearts to Stratify Arrhythmia Risk in Post-MI Patients

In this application of the virtual heart approach to post-MI patients, the multi-site delivery of ventricular stimuli was used to determine the patient's heart propensity to develop infarct-related ventricular arrhythmias. Arevalo et al[17] termed this non-invasive SCD risk assessment approach VARP, Virtual-heart Arrhythmia Risk Predictor. Since the goal of electrically "stressing out" the ventricular substrate is to only determine presence of reentrant arrhythmia (or the lack thereof) as the result of pacing from at least one site, this application is conceptually simpler and less computationally demanding than the ablation guidance described above, allowing for evaluation of the predictive capability of the approach in a larger patient cohort, and for comparison with other clinical metrics.

The retrospective proof-of-concept study by Arevalo et al[17] used data from 41 patients with prior MI and LVEF<35%, chosen randomly from those enrolled in the CMR-Prospective Observational Study of Implantable Cardioverter Defibrillators (CMR-PROSE-ICD)[48]. Patients were followed for the primary end point of appropriate ICD firing due to ventricular arrhythmia or cardiac death. Follow-up time averaged 4.8 ± 2.9 years. VARP predictive capabilities were compared to LVEF as well as to other clinical metrics that have been used

to predict arrhythmic risk, such as GZ volume[49], scar volume[50] and LV mass[51]. Furthermore, 32 of the 41 patients in the cohort underwent, at the time of ICD implantation, clinical electrophysiological testing; for these 32 patients, VARP assessment was also compared with the outcome of the clinical testing. Figure 7 presents 7 reconstructed patient heart models; induced arrhythmia is shown in 2 models (transmembrane potential and activation maps), with reentrant waves often propagating through isthmuses in the scar. In the five models shown at Figure 7, bottom, no arrhythmia was induced from any pacing site, despite the presence of infarcted tissue.

Statistical analysis[17] demonstrated that a positive VARP test was significantly associated with the primary end point, with a four-fold higher arrhythmia risk than patients with negative VARP test. The comparison of VARP with LVEF, as well as with GZ volume, scar volume and LV mass, revealed that only VARP outcome was significantly associated with arrhythmic risk in this small cohort. When only appropriate ICD shock was used as a secondary end point, the hazard ratio for VARP increased from 4.05 to 5.0. Among the 32 patients who had both VARP and invasive testing, the hazard ratio for VARP was 10.4 versus 1.7 for clinical electrophysiological testing. For the appropriate shock end point, the hazard ratio for VARP remained significant at 8.60, versus 2.60 for clinical testing. It is important to note that the non-invasive nature of VARP offers an additional advantage over clinical testing, which entails risks of vascular access, sedation and induction of ventricular arrhythmias requiring defibrillation in already tenuous cardiomyopathy patients.

The superiority of the VARP approach, as demonstrated by Arevalo et al[17], stems from its ability to comprehensively evaluate the arrhythmogenic propensity of the MI substrate as probed by triggers acting at locations of different geometrical position with respect to remodeled tissue. Should the predictive capability of the approach be demonstrated in larger studies, VARP has the potential to radically change the process of SCD risk assessment and patient selection for prophylactic ICD implantation, potentially eliminating many unnecessary ICD implantations and their associated complications (infections, device malfunctions and inappropriate shocks).

Importantly, as acknowledged by Arevalo et al[17], VARP could be applied to patients with prior MI but preserved LVEF>30–35%, who could also be at significant risk for arrhythmia because of their remodeled myocardium, but are generally not targeted for therapy under current clinical recommendations[52]. Because current guidelines for ICD placement target low LVEF patients who constitute only one-third of SCD victims[53], VARP has the potential to identify increased SCD risk in a much larger number of at-risk patients. The first step in this direction was recently made by Deng et al[33], who applied VARP in the analysis of data from 4 patients with MI and average LVEF of 44.0 ± 2.6%. VARP correctly predicted the occurrence of VT in one patient and the lack thereof in the remaining three, as shown in Figure 8.

Concluding Remarks and Outlook

The immense potential of simulation-driven applications in cardiac patient care has been recognized in a number of recent reviews[54,55], arguing that clinical translation of

physiological models will transform medical practice. However, getting to the point of translation is a long road, and success has been variable depending on the specific applications. In this review, we examined recent advances in using physics-based physiological models in the diagnosis and treatment of cardiac arrhythmias. Initial applications have focused on structural heart disease, necessitating the development of geometric models from clinical images so that structural remodeling of the ventricular substrate could be adequately represented. It is important to note that these models do not and cannot fully reflect the biology of remodeling. The goal is to create a clinically useful tool, which, while having mechanistic underpinnings, can also be successfully used in the clinic to improve diagnostics (SCD risk) or non-invasively guide therapies (VT ablation). This requires a balance between model execution time and the level of model detail. As further progress is made, such balance will need to be disease-specific, and decisions regarding model complexity will need to be made within the constraints of the given clinical application.

While initial successes of the virtual heart approach provide a glimpse into the potential of the technology, its development to full potential and utilization in the clinic are dependent on a number of current limiting factors; overcoming these will ensure easy and straightforward implementation in the clinic. Some of these include:

- *Contrast-enhanced image quality and standardization*. The quality and resolution of clinical images is paramount to image-based model construction. Improvements in the quality of cardiac MR and standardization of image acquisition across clinical centers will ensure consistently high quality of the patient-specific virtual hearts. Alternatively, CT scans could be used, should there be a possibility for acquiring contrast-enhanced images of remodeled heart structure at high signal-to-noise ratio.
- *Accelerated image processing with minimum manual input*. Image processing of clinical-quality cardiac scans is a dynamic field, with major advancements made particularly in reconstructing ventricular shape over just minutes. Reconstruction of enhanced regions of remodeling has seen less advancement, but remains crucial to model construction, and in need of new algorithms that will decrease time and manual input.
- *Algorithmic developments to decrease model execution times.* The need to execute calculations of VT circuits and ablation targets in a limited interval of time consistent with procedure and patient care timelines imposes major constraints on the simulation process, as the electrophysiological simulation code is computationally demanding. Additional speed up and development of lightweight application-adjusted electrophysiological simulators would relieve this burden.

Further developments of the virtual heart approach are expected to extend to diagnosis and arrhythmia risk stratification in other disease conditions, such as Tetralogy of Fallot and non-ischemic and hypertrophic cardiomyopathies, as recent preliminary data demonstrate[56,57]. Importantly, the approach is also extendable to predicting ablation targets for atrial arrhythmias. A retrospective study[46] using the virtual heart approach to predict

targets for atypical atrial flutter ablation in 10 patients with atrial fibrotic remodeling demonstrated excellent correspondence to clinical targets. Finally, while the approach has not yet been utilized to find ablation targets for persistent atrial fibrillation (AF), a recent study by Zahid et al[58] demonstrated the ability to create atrial patient-specific models from CMR-LGE scans that predicted AF reentrant drivers consistent with clinical recordings. Advancements in the virtual heart methodology and its applications could thus help usher a number of personalized medicine approaches in cardiac patient care.

Acknowledgments

Sources of Funding: The authors acknowledge support by the National Institutes of Health Director's Pioneer Award to NT (DP1HL123271).

References

1. Hood L, Heath JR, Phelps ME, Lin B. Systems biology and new technologies enable predictive and preventative medicine. Science. 2004; 306:640–643. [PubMed: 15499008]
2. Schadt EE, Björkegren JLM. NEW: network-enabled wisdom in biology, medicine, and health care. Sci Transl Med. 2012; 4:115rv1–115rv1.
3. Winslow RL, Trayanova N, Geman D, Miller MI. Computational Medicine: Translating Models to Clinical Care. Sci Transl Med. 2012; 4:158rv11–158rv11.
4. Fishman GI, Chugh SS, DiMarco JP, Albert CM, Anderson ME, Bonow RO, Buxton AE, Chen PS, Estes M, Jouven X. Sudden cardiac death prediction and prevention. Circulation. 2010; 122:2335–2348. [PubMed: 21147730]
5. Goldberger Z, Lampert R. Implantable cardioverter-defibrillators: expanding indications and technologies. JAMA. 2006; 295:809–818. [PubMed: 16478904]
6. Bardy GH, Lee KL, Mark DB, Poole JE, Packer DL, Boineau R, Domanski M, Troutman C, Anderson J, Johnson G. Amiodarone or an implantable cardioverter–defibrillator for congestive heart failure. N Engl J Med. 2005; 352:225–237. [PubMed: 15659722]
7. Reynolds MR, Cohen DJ, Kugelmass AD, Brown PP, Becker ER, Culler SD, Simon AW. The frequency and incremental cost of major complications among medicare beneficiaries receiving implantable cardioverter-defibrillators. J Am Coll Cardiol. 2006; 47:2493–2497. [PubMed: 16781379]
8. Stevenson WG, Friedman PL, Kocovic D, Sager PT, Saxon LA, Pavri B. Radiofrequency catheter ablation of ventricular tachycardia after myocardial infarction. Circulation. 1998; 98:308–314. [PubMed: 9711935]
9. Aliot EM, Stevenson WG, Almendral-Garrote JM, Bogun F, Calkins CH, Delacretaz E, Della Bella P, Hindricks G, Jaïs P, Josephson ME. EHRA/HRS expert consensus on catheter ablation of ventricular arrhythmias. Europace. 2009; 11:771–817. [PubMed: 19443434]
10. Calkins H, Epstein A, Packer D, Arria AM, Hummel J, Gilligan DM, Trusso J, Carlson M, Luceri R, Kopelman H. Catheter ablation of ventricular tachycardia in patients with structural heart disease using cooled radiofrequency energy: results of a prospective multicenter study. J Am Coll Cardiol. 2000; 35:1905–1914. [PubMed: 10841242]
11. Zhong H, Lacomis JM, Schwartzman D. On the accuracy of CartoMerge for guiding posterior left atrial ablation in man. Heart Rhythm. 2007; 4:595–602. [PubMed: 17467627]
12. Sosa E, Scanavacca M, d'Avila A, Oliveira F, Ramires JAF. Nonsurgical transthoracic epicardial catheter ablation to treat recurrent ventricular tachycardia occurring late after myocardial infarction. J Am Coll Cardiol. 2000; 35:1442–1449. [PubMed: 10807445]
13. Dong J, Dalal D, Scherr D, Cheema A, Nazarian S, Bilchick K, Almasry I, Cheng A, Henrikson CA, Spragg D. Impact of heart rhythm status on registration accuracy of the left atrium for catheter ablation of atrial fibrillation. J Cardiovasc Electrophysiol. 2007; 18:1269–1276. [PubMed: 17850289]

14. de Bakker JM, van Capelle FJ, Janse MJ, Wilde AA, Coronel R, Becker AE, Dingemans KP, van Hemel NM, Hauer RN. Reentry as a cause of ventricular tachycardia in patients with chronic ischemic heart disease: electrophysiologic and anatomic correlation. Circulation. 1988; 77:589–606. [PubMed: 3342490]
15. Peters NS, Wit AL. Myocardial architecture and ventricular arrhythmogenesis. Circulation. 1998; 97:1746–1754. [PubMed: 9591770]
16. Tung R, Josephson ME, Reddy V, Reynolds MR. Influence of Clinical and Procedural Predictors on Ventricular Tachycardia Ablation Outcomes: An Analysis From the Substrate Mapping and Ablation in Sinus Rhythm to Halt Ventricular Tachycardia Trial (SMASH-VT). J Cardiovasc Electrophysiol. 2010; 21:799–803. [PubMed: 20132389]
17. Arevalo HJ, Vadakkumpadan F, Guallar E, Jebb A, Malamas P, Wu KC, Trayanova NA. Arrhythmia risk stratification of patients after myocardial infarction using personalized heart models. Nat Commun. 2016; 7:11437. [PubMed: 27164184]
18. Prakosa A, Malamas P, Zhang S, Pashakhanloo F, Arevalo H, Herzka DA, Lardo A, Halperin H, McVeigh E, Trayanova N, Vadakkumpadan F. Methodology for image-based reconstruction of ventricular geometry for patient-specific modeling of cardiac electrophysiology. Prog Biophys Mol Biol. 2014; 115:226–234. [PubMed: 25148771]
19. Prakosa, A., Nikolov, P., Zahid, S., Ipek, EG., Nazarian, S., Trayanova, NA. Feasibility of Simulation-Based Prediction of Optimal Ventricular Tachycardia (VT) Ablation Targets in Patients With ICD Artifact Burden. 2016.
20. Ranjan R, Kholmovski EG, Jeong E-K, Hong K, Blauer J, Wilson BD, McGann CJ, Kim D. Off-resonance insensitive LGE MRI for imaging ventricular scar without image artifacts induced by cardiac devices. J Cardiovasc Magn Reson. 2014; 16(Suppl 1):O54.
21. Schmidt A, Azevedo CF, Cheng A, Gupta SN, Bluemke DA, Foo TK, Gerstenblith G, Weiss RG, Marbán E, Tomaselli GF, Lima JA, Wu KC, David A. Infarct tissue heterogeneity by magnetic resonance imaging identifies enhanced cardiac arrhythmia susceptibility in patients with left ventricular dysfunction. Circulation. 2007; 115:2006–2014. [PubMed: 17389270]
22. Ukwatta E, Arevalo H, Li K, Yuan J, Qiu W, Malamas P, Wu KC, Trayanova NA, Vadakkumpadan F. Myocardial Infarct Segmentation from Magnetic Resonance Images for Personalized Modeling of Cardiac Electrophysiology. IEEE Trans Med Imaging. 2016; 35:1408–1419. [PubMed: 26731693]
23. Ukwatta E, Arevalo H, Rajchl M, White J, Pashakhanloo F, Prakosa A, Herzka DA, Mcveigh E, Lardo AC, Trayanova NA, Vadakkumpadan F, White J. Image-based reconstruction of three-dimensional myocardial infarct geometry for patient-specific modeling of cardiac electrophysiology. Med Phys. 2015; 42:4579–4590. [PubMed: 26233186]
24. Prassl AJ, Kickinger F, Ahammer H, Grau V, Schneider JE, Hofer E, Vigmond EJ, Trayanova NA, Plank G. Automatically generated, anatomically accurate meshes for cardiac electrophysiology problems. IEEE Trans Biomed Eng. 2009; 56:1318–1330. [PubMed: 19203877]
25. Gurev V, Lee T, Constantino J, Arevalo H, Trayanova NA. Models of cardiac electromechanics based on individual hearts imaging data: Image-based electromechanical models of the heart. Biomech Model Mechanobiol. Jun.2011 10:295–306. [PubMed: 20589408]
26. Nielles-Vallespin S, Khalique Z, Ferreira PF, de Silva R, Scott AD, Kilner P, McGill L, Giannakidis A, Gatehouse PD, Ennis D, De Silva R, Scott AD, Kilner P, McGill L, Giannakidis A, Gatehouse PD, Ennis D, Aliotta E, Al-khalil M, Kellman P, Mazilu D, Balaban RS, Firmin DN, Arai AE, Pennell DJ. Assessment of myocardial microstructural dynamics by in vivo diffusion tensor cardiac magnetic resonance. J Am Coll Cardiol. 2017; 69:661–676. [PubMed: 28183509]
27. Vadakkumpadan F, Arevalo H, Ceritoglu C, Miller M, Trayanova N. Image-based estimation of ventricular fiber orientations for personalized modeling of cardiac electrophysiology. IEEE Trans Med Imaging. 2012; 31:1051–1060. [PubMed: 22271833]
28. Ringenberg J, Deo M, Filgueiras-Rama D, Pizarro G, Ibañez B, Peinado R, Trayanova N, Miller M, l Merino J, Berenfeld O. Corrigendum to “Effects of Fibrosis Morphology on Reentrant Ventricular Tachycardia Inducibility and Simulation Fidelity in Patient-Derived Models. ” Clin Med Insights Cardiol. 2014; 8:51.

29. Bayer JD, Blake RC, Plank G, Trayanova NA. A novel rule-based algorithm for assigning myocardial fiber orientation to computational heart models. Ann Biomed Eng. 2012; 40:2243–2254. [PubMed: 22648575]
30. Pashakhanloo F, Herzka DA, Mori S, Zviman M, Halperin H, Gai N, Bluemke DA, Trayanova NA, Mcveigh ER. Submillimeter diffusion tensor imaging and late gadolinium enhancement cardiovascular magnetic resonance of chronic myocardial infarction. J Cardiovasc Magn Reson. 2017; 19:9. [PubMed: 28122618]
31. Arevalo H, Plank G, Helm P, Halperin H, Trayanova N. Tachycardia in post-infarction hearts: insights from 3D image-based ventricular models. PLoS One. 2013; 8:e68872. [PubMed: 23844245]
32. Deng D, Arevalo H, Pashakhanloo F, Prakosa A, Ashikaga H, McVeigh E, Halperin H, Trayanova N. Accuracy of prediction of infarct-related arrhythmic circuits from image-based models reconstructed from low and high resolution MRI. Front Physiol. 2015; 6:1–12. [PubMed: 25688210]
33. Deng D, Arevalo HJ, Prakosa A, Callans DJ, Trayanova NA. A feasibility study of arrhythmia risk prediction in patients with myocardial infarction and preserved ejection fraction. Europace. 2016; 18:iv60–iv66. [PubMed: 28011832]
34. Plank G, Zhou L, Greenstein JL, Cortassa S, Winslow RL, O'Rourke B, Trayanova Na. From mitochondrial ion channels to arrhythmias in the heart: computational techniques to bridge the spatio-temporal scales. Philos Trans A Math Phys Eng Sci. 2008; 366:3381–3409. [PubMed: 18603526]
35. Rodriguez B, Li L, Eason JC, Efimov IR, Trayanova NA. Differences between left and right ventricular chamber geometry affect cardiac vulnerability to electric shocks. Circ Res. 2005; 97:168–175. [PubMed: 15976315]
36. Rantner LJ, Arevalo HJ, Constantino JL, Efimov IR, Plank G, Trayanova NA. Three-dimensional mechanisms of increased vulnerability to electric shocks in myocardial infarction: Altered virtual electrode polarizations and conduction delay in the peri-infarct zone. J Physiol. 2012; 590:4537–4551. [PubMed: 22586222]
37. Bishop MJ, Rodriguez B, Qu F, Efimov IR, Gavaghan DJ, Trayanova NA. The role of photon scattering in optical signal distortion during arrhythmia and defibrillation. Biophys J. 2007; 93:3714–3726. [PubMed: 17978166]
38. Priest JR, Gawad C, Kahlig KM, Joseph KY, O'Hara T, Boyle PM, Rajamani S, Clark MJ, Garcia STK, Ceresnak S, Rush J, Gawad C, Kahlig KM, Yu JK, Hara TO, Boyle PM. Early somatic mosaicism is a rare cause of long-QT syndrome. Proc Natl Acad Sci. 2016; 113:11555–11560. [PubMed: 27681629]
39. Bruegmann T, Boyle PM, Vogt CC, Karathanos TV, Arevalo HJ, Fleischmann BK, Trayanova NA, Sasse P. Optogenetic defibrillation terminates ventricular arrhythmia in mouse hearts and human simulations. J Clin Invest. 2016; 126:3894–3904. [PubMed: 27617859]
40. Moreno JD, Zhu ZI, Yang P-C, Bankston JR, Jeng M-T, Kang C, Wang L, Bayer JD, Christini DJ, Trayanova NA. A computational model to predict the effects of class I anti-arrhythmic drugs on ventricular rhythms. Sci Transl Med. 2011; 3:98ra83–98ra83.
41. Pop M, Sermesant M, Mansi T, Crystal E, Ghate S, Peyrat J-M, Lashevsky I, Qiang B, McVeigh E, Ayache N, Wright GA. Correspondence between simple 3-D MRI-based computer models and in-vivo EP measurements in swine with chronic infarctions. IEEE Trans Biomed Eng. 2011; 58:3483–3486. [PubMed: 21926012]
42. Relan J, Chinchapatnam P, Sermesant M, Rhode K, Ginks M, Delingette H, Rinaldi CA, Razavi R, Ayache N, Rhode K, Ginks M. Coupled personalization of cardiac electrophysiology models for prediction of ischaemic ventricular tachycardia. Interface Focus. 2011; 1:396–407. [PubMed: 22670209]
43. Chen Z, Cabrera-Lozoya R, Relan J, Sohal M, Shetty A, Karim R, Delingette H, Gill J, Rhode K, Ayache N. Biophysical Modeling Predicts Ventricular Tachycardia Inducibility and Circuit Morphology: A Combined Clinical Validation and Computer Modeling Approach. J Cardiovasc Electrophysiol. 2016; 27:851–860. [PubMed: 27094470]

44. Ranjan R, Ghafoori E, Blauer J, Dongdong D, Arevalo H, Prakosa A, Han F, Wall S, Freedman R, Mcgarry T. Personalized MRI-Based Modeling Predicts Ventricular Tachycardia Vulnerability in Patients Receiving Primary Prevention ICDs. Circ. 2016; 134(Suppl 1):A16247–A16247.
45. Ashikaga H, Arevalo H, Vadakkumpadan F, Blake RC, Bayer JD, Nazarian S, Muz Zviman M, Tandri H, Berger RD, Calkins H, Herzka DA, Trayanova NA, Halperin HR. Feasibility of image-based simulation to estimate ablation target in human ventricular arrhythmia. Heart Rhythm. 2013; 10:1109–1116. [PubMed: 23608593]
46. Zahid S, Whyte KN, Schwarz EL, Blake RC III, Boyle PM, Chrispin J, Prakosa A, Ipek EG, Pashakhanloo F, Halperin HR, Calkins H, Berger RD, Nazarian S, Trayanova NA. Feasibility of using patient-specific models and the "minimum cut" algorithm to predict optimal ablation targets for left atrial flutter. Heart Rhythm. 2016; 13:1687–1698. [PubMed: 27108938]
47. Dickfeld T, Kato R, Zviman M, Lai S, Meininger G, Lardo AC, Roguin A, Bluemke D, Berger R, Calkins H. Characterization of radiofrequency ablation lesions with gadolinium-enhanced cardiovascular magnetic resonance imaging. J Am Coll Cardiol. 2006; 47:370–378. [PubMed: 16412863]
48. Wu KC, Gerstenblith G, Guallar E, Marine JE, Dalal D, Cheng A, Marbán E, Lima JAC, Tomaselli GF, Weiss RG. Combined Cardiac Magnetic Resonance Imaging and C-Reactive Protein Levels Identify a Cohort at Low Risk for Defibrillator Firings and Death Clinical Perspective. Circ Cardiovasc Imaging. 2012; 5:178–186. [PubMed: 22267750]
49. Roes SD, Borleffs CJW, Van Der Geest RJ, Westenberg JJM, Marsan NA, Kaandorp TAM, Reiber JHC, Zeppenfeld K, Lamb HJ, De Roos A, Schalij MJ, Bax JJ. Infarct tissue heterogeneity assessed with contrast-enhanced mri predicts spontaneous ventricular arrhythmia in patients with ischemic cardiomyopathy and implantable cardioverter-defibrillator. Circ Cardiovasc Imaging. 2009; 2:183–190. [PubMed: 19808591]
50. Klem I, Weinsaft JW, Bahnson TD, Hegland D, Kim HW, Hayes B, Parker MA, Judd RM, Kim RJ. Assessment of myocardial scarring improves risk stratification in patients evaluated for cardiac defibrillator implantation. J Am Coll Cardiol. 2012; 60:408–420. [PubMed: 22835669]
51. Haider AW, Larson MG, Benjamin EJ, Levy D. Increased left ventricular mass and hypertrophy are associated with increased risk for sudden death. J Am Coll Cardiol. 1998; 32:1454–1459. [PubMed: 9809962]
52. Gorgels APM, Gijsbers C, de Vreede-Swagemakers J, Lousberg A, Wellens HJJ. Out-of-hospital cardiac arrest-the relevance of heart failure. The Maastricht Circulatory Arrest Registry. Eur Heart J. 2003; 24:1204–1209. [PubMed: 12831814]
53. Stecker EC, Vickers C, Waltz J, Socoteanu C, John BT, Mariani R, McAnulty JH, Gunson K, Jui J, Chugh SS. Population-based analysis of sudden cardiac death with and without left ventricular systolic dysfunction: two-year findings from the Oregon Sudden Unexpected Death Study. J Am Coll Cardiol. 2006; 47:1161–1166. [PubMed: 16545646]
54. Hill AP, Perry MD, Abi-Gerges N, Couderc JJ, Fermini B, Hancox JC, Knollmann BC, Mirams GR, Skinner J, Zareba W, Abi-gerges N, Couderc JJ, Fermini B, Hancox JC, Knollmann BC, Mirams GR, Skinner J, Zareba W, Vandenberg JI. Computational cardiology and risk stratification for sudden cardiac death: one of the grand challenges for cardiology in the 21st century. J Physiol. 2016; 594:6893–6908. [PubMed: 27060987]
55. Niederer SA, Smith NP. Using physiologically based models for clinical translation: predictive modelling, data interpretation or something in-between? J Physiol. 2016; 594:6849–6863. [PubMed: 27121495]
56. Cartoski MJ, Prakosa A, Nikolov P, Boyle PM, Spevak PJ, Trayanova N. Risk Stratification for Ventricular Arrhythmia in Patients With Repaired Tetralogy of Fallot (TOF) via Image-Based Computational Simulations: A Pilot Study. Circ. 2016; 134(Suppl 1):A11921–A11921.
57. Nikolov P, Prakosa A, Arevalo HJ, Wu KC, Trayanova N. A Novel Approach to Arrhythmia Risk Stratification in Patients With Non-ischemic Cardiomyopathy. Circ. 2016; 134(Suppl 1):A20903–A20903.
58. Zahid S, Cochet H, Boyle PM, Schwarz EL, Whyte KN, Vigmond EJ, Dubois R, Hocini M, Haïssaguerre M, Jaïs P, Trayanova NA. Patient-derived models link reentrant driver localization in atrial fibrillation to fibrosis spatial pattern. Cardiovasc Res. 2016; 110:443–454. [PubMed: 27056895]

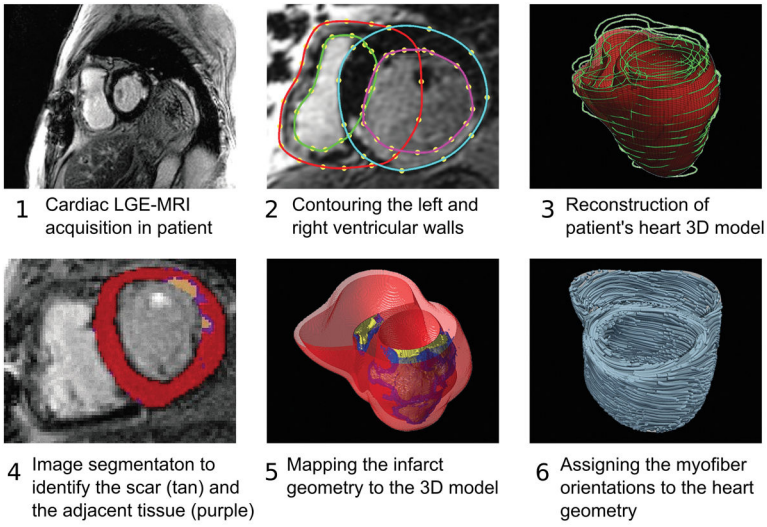

Figure 1.
Pipeline for construction of patient's heart model.

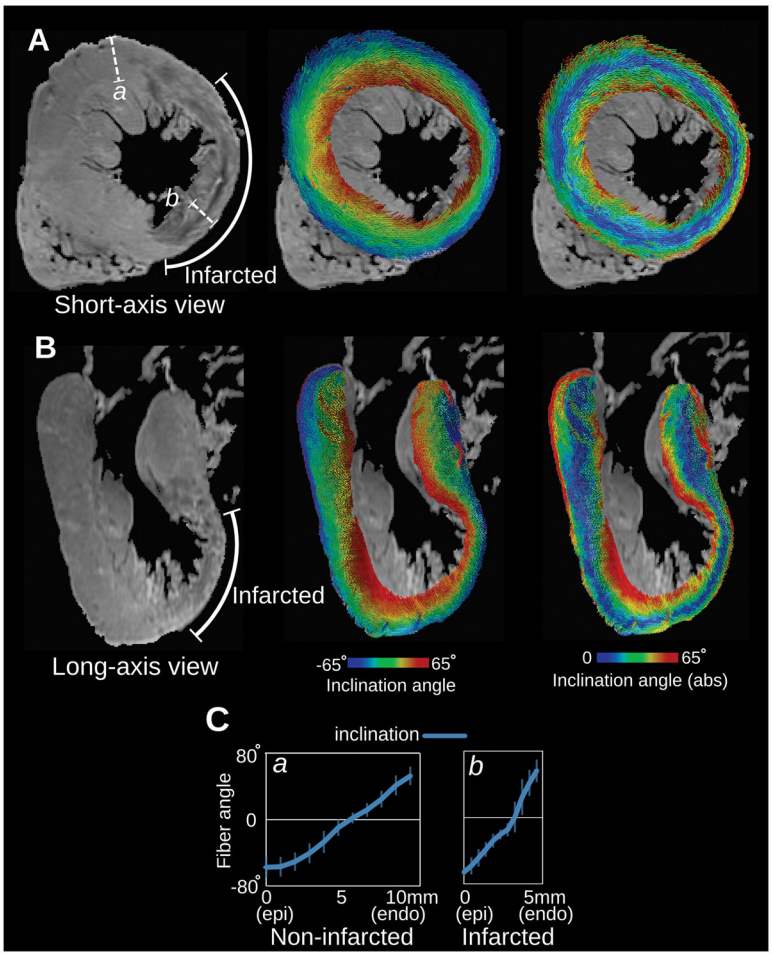

Figure 2.

Fiber visualization in a human LV with MI, obtained from *ex vivo* sub-millimeter DT MRI. **A,** short-axis and **B,** long axis view of the non-diffusion-weighted image (*left*), primary eigenvector visualizations color-coded with inclination angle (*middle*), and absolute value of inclination angle (*right*). The infarcted wall is identifiable by the wall thinning at the LV anterioapical region as observed in the non-diffusion-weighted images. **C** Transmural angle profiles measured in two segments from non-infarcted and infarcted regions (*a* and *b* in panel **A** *left*). Modified from Pashakhanloo et al[30] under the Creative Commons license.

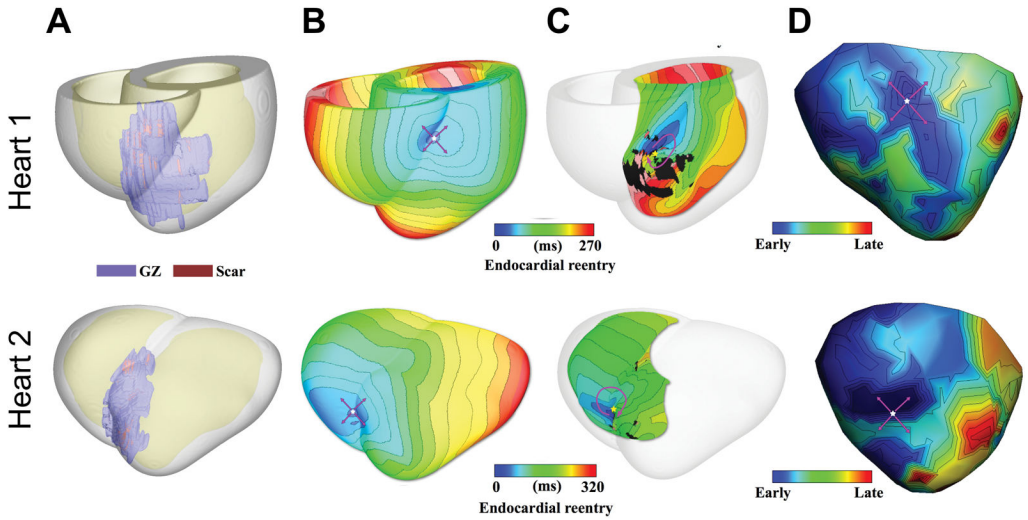

Figure 3.

Comparison of simulation and experimental results in two infarcted pig hearts. **A,** Reconstructed models with the epicardium rendered semi-transparent. Scar and GZ appear in red and purple, respectively. **B,** Activation maps of simulated VTs with breakthrough patterns on the epicardium. **C,** Endocardial views showing reentrant source. **D,** Experimentally recorded epicardial activation map. Pink arrows denote propagation direction. Modified from Deng et al[32] under the Creative Commons license.

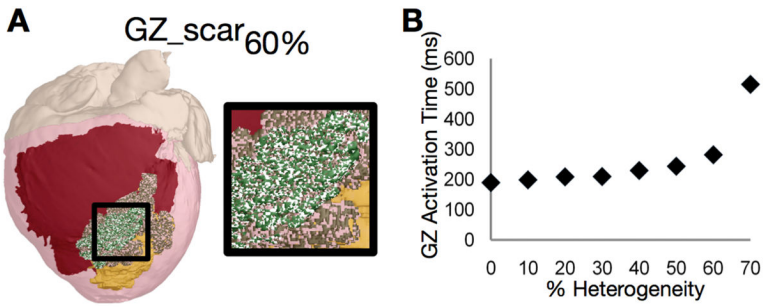

Figure 4.

Sensitivity of electrical activity in the canine ventricular model to GZ electrophysiological properties. **A,** Model with 60% scar in GZ (white speckles). Myocardium is colored in red, scar and GZ are yellow and green, respectively. **B,** Time needed to fully activate GZ by propagation as a function of scar density in GZ. Reused from Arevalo et al[31] under the Creative Commons license.

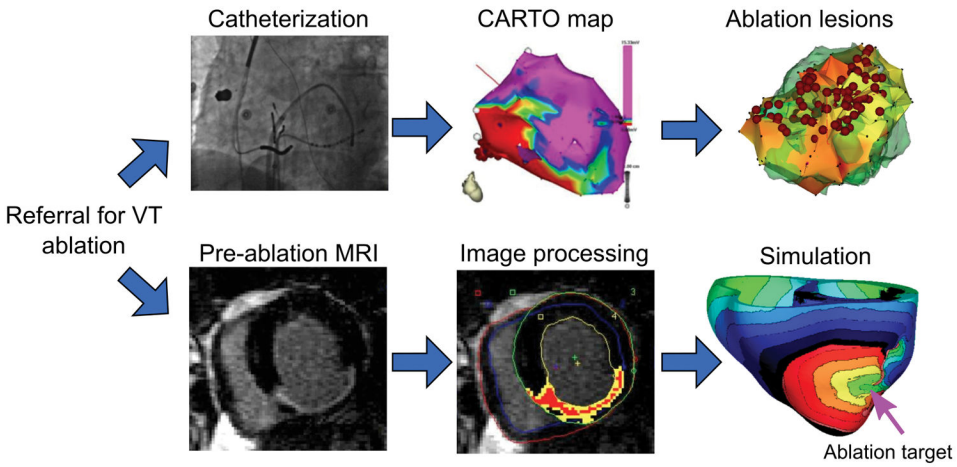

Figure 5.
VT ablation workflows for (top) standard approach and (bottom) image-based simulation approach.

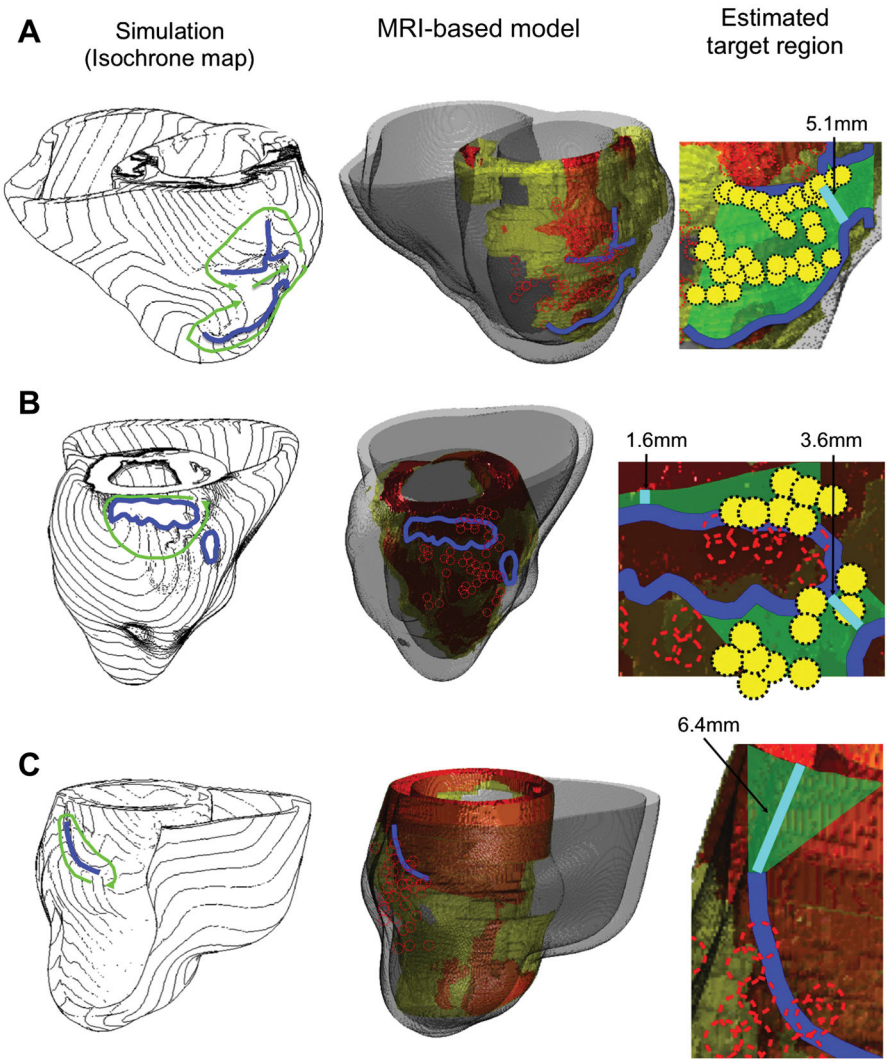

Figure 6.

MRI-based simulation approach for estimating infarct-related VT ablation targets. Each row represents a different patient (A–C). The Simulation column shows calculated isochrone maps of VT. Green arrows indicate direction of propagation. Lines of conduction block are in blue. MRI-based model column presents models constructed from pre-ablation MRIs (scar: orange; GZ: yellow; non-infarcted myocardium: gray). The lines of conduction block (blue lines) from the simulations and the ablation sites (red circles) from the clinical approach are co-registered on the model geometry. The Estimated target region column shows a potential target region (green area) estimated from the simulations. The shortest possible line of ablation that spans the target region (i.e., narrowest width of the isthmus) is shown in cyan color. Clinical ablation sites that fell within the green area are indicated by yellow circles. The first 2 simulation results in this figure (patients A and B) show a figure-of-eight pattern, and the last simulation result (patient C) show a unidirectional reentry. Modified with permission from Ashikaga et al[45].

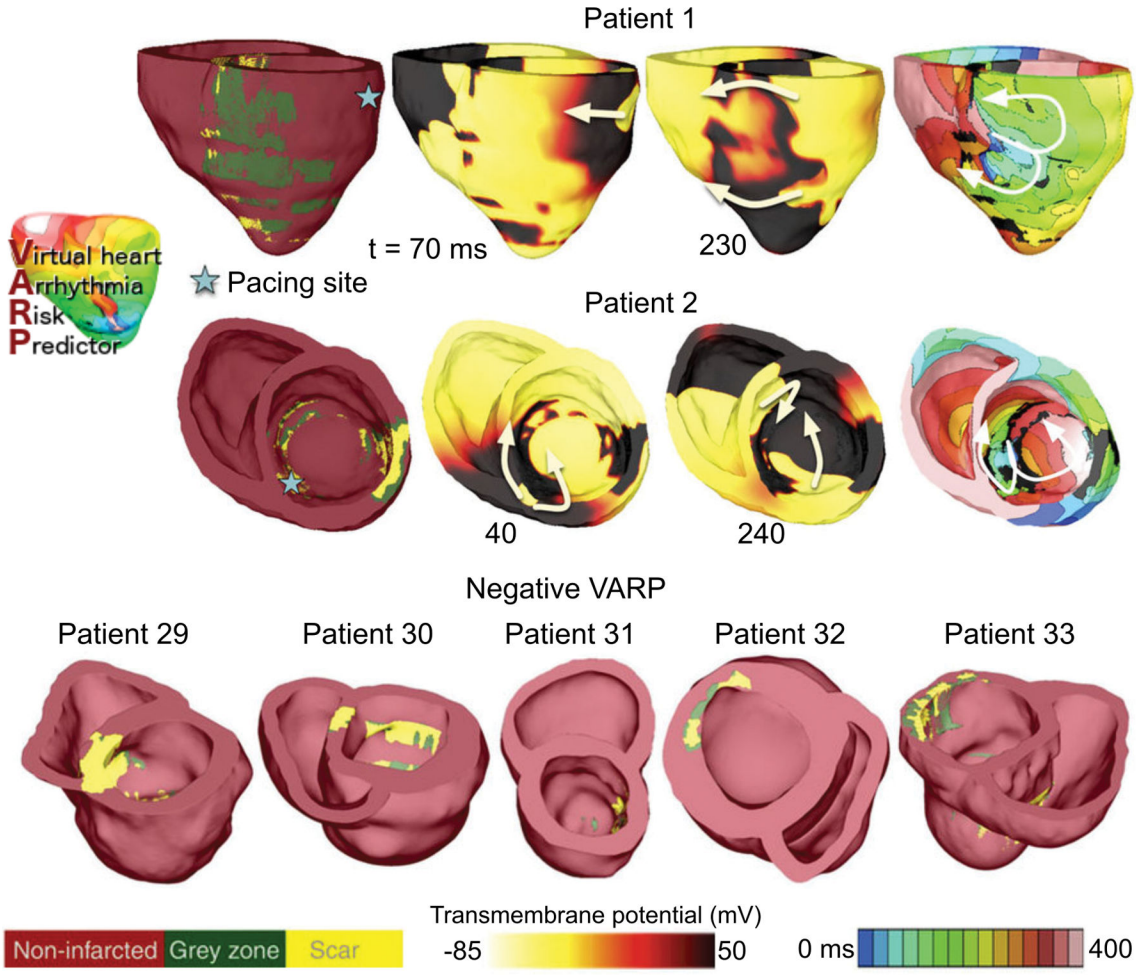

Figure 7.

Illustrative examples of VARP results for 7 of the 41 personalized heart models. Induced arrhythmia in two hearts are shown (top), for which geometrical models are presented together with transmembrane voltage and electrical activation isochronal maps, obtained following pacing from the site indicated. White arrows represent direction of propagation of the reentrant arrhythmias. The geometrical models of the five hearts, in which no arrhythmia was induced from any pacing site, are shown at the bottom. Modified from Arevalo et al[17] under the Creative Commons license.

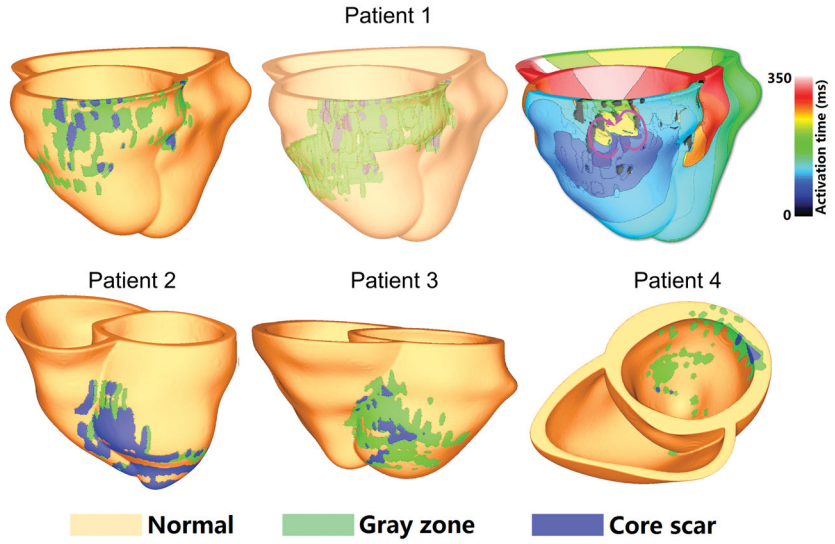

Figure 8.

Ventricular models for 4 patients with MI and preserved LVEF. Virtual heart from patient 1 (top row; model shown on left and in semi-transparent view in middle) had inducible VT (isochronal map top right; purple arrows show direction of propagation of reentrant arrhythmia). Models from patients 2–4 (bottom row) demonstrated no inducible arrhythmia. Modified with permission from Deng et al[33].